


Methylene blue prevents retinal damage in an experimental model of ischemic proliferative retinopathy

Manuel Rey-Funes,^{1*}  Ignacio M. Larrayoz,^{2*} Juan C. Fernández,³ Daniela S. Contartese,¹ Federico Rolón,¹ Pablo I. F. Inserra,⁴ Ricardo Martínez-Murillo,⁵ Juan J. López-Costa,¹ Verónica B. Dorfman,⁴ Alfredo Martínez,² and César F. Loidl^{1,6}

¹Laboratorio de Neuropatología Experimental, Instituto de Biología Celular y Neurociencia “Prof. E. De Robertis,” Facultad de Medicina, Universidad de Buenos Aires, Consejo Nacional de Investigaciones Científicas y Técnicas, Buenos Aires, Argentina; ²Angiogenesis Study Group, Center for Biomedical Research of La Rioja, Logroño, Spain; ³Primera Cátedra de Farmacología, Facultad de Medicina, Universidad de Buenos Aires, Buenos Aires, Argentina; ⁴Centro de Estudios Biomédicos, Biotecnológicos, Ambientales y Diagnóstico, Universidad Maimónides, Buenos Aires, Argentina; ⁵Neurovascular Research Group, Department of Molecular, Cellular and Developmental Neurobiology, Instituto Cajal, Consejo Superior Investigaciones Científicas, Madrid, Spain; and ⁶Laboratorio de Neurociencia, Facultad de Ciencias Médicas, Universidad Católica de Cuyo, San Juan, Argentina

Submitted 12 June 2015; accepted in final form 11 March 2016

Rey-Funes M, Larrayoz IM, Fernández JC, Contartese DS, Rolón F, Inserra PI, Martínez-Murillo R, López-Costa JJ, Dorfman VB, Martínez A, Loidl CF. Methylene blue prevents retinal damage in an experimental model of ischemic proliferative retinopathy. *Am J Physiol Regul Integr Comp Physiol* 310: R1011–R1019, 2016. First published March 16, 2016; doi:10.1152/ajpregu.00266.2015.—Perinatal asphyxia induces retinal lesions, generating ischemic proliferative retinopathy, which may result in blindness. Previously, we showed that the nitric system was involved in the physiopathology of perinatal asphyxia. Here we analyze the application of methylene blue, a well-known soluble guanylate cyclase inhibitor, as a therapeutic strategy to prevent retinopathy. Male rats ($n = 28$ per group) were treated in different ways: 1) control group comprised born-to-term animals; 2) methylene blue group comprised animals born from pregnant rats treated with methylene blue (2 mg/kg) 30 and 5 min before delivery; 3) perinatal asphyxia (PA) group comprised rats exposed to perinatal asphyxia (20 min at 37°C); and 4) methylene blue–PA group comprised animals born from pregnant rats treated with methylene blue (2 mg/kg) 30 and 5 min before delivery, and then the pups were subjected to PA as above. For molecular studies, mRNA was obtained at different times after asphyxia, and tissue was collected at 30 days for morphological and biochemical analysis. Perinatal asphyxia produced significant gliosis, angiogenesis, and thickening of the inner retina. Methylene blue treatment reduced these parameters. Perinatal asphyxia resulted in a significant elevation of the nitric system as shown by NO synthase (NOS) activity assays, Western blotting, and (immuno)histochemistry for the neuronal isoform of NOS and NADPH-diaphorase activity. All these parameters were also normalized by the treatment. In addition, methylene blue induced the upregulation of the anti-angiogenic peptide, pigment epithelium-derived factor. Application of methylene blue reduced morphological and biochemical parameters of retinopathy. This finding suggests the use of methylene blue as a new treatment to prevent or decrease retinal damage in the context of ischemic proliferative retinopathy.

retina; nitric oxide; ischemic proliferative retinopathy; methylene blue; angiogenesis

PERINATAL ASPHYXIA (PA) is one of the most severe problems in perinatology services across the world (9, 15, 23, 27). PA

generates a transient global hypoxia-ischemia status that damages the brain, spinal cord, and retina (14, 17, 39, 52). The degree and the length of perinatal asphyxia are decisive for the development of injury sequelae, such as attention-deficit hyperactivity disorder (1), epilepsy, mental retardation, spasticity, and visual or hearing alterations (61). One third of asphyctic neonates develop serious long-term neurological injuries including several degrees of ischemic proliferative retinopathy (IPR) and even blindness (20).

In rats, the retina is particularly sensitive to oxygen alterations (56), and the morphological changes observed in its inner layers are compatible with some alterations observed in human diseases such as retinopathy in diabetes, retinal vein occlusion, and retinopathy of prematurity (ROP), an avoidable cause of visual impairment and blindness in children (20, 61). The changes observed in asphyctic animals include ganglion cell degeneration, neovascularization of the innermost layers of the retina (the internal limiting membrane, the retinal nerve fiber layer, and the ganglion cell layer), and Müller cell hypertrophy in the inner layers of the retina (including the inner nuclear layer, the inner plexiform layer, the ganglion cell layer, the retinal nerve fiber layer, and the internal limiting membrane) (44). Therefore, in rodents, it makes sense to use the term ischemic proliferative retinopathy to describe these changes.

Several mechanisms have been involved in PA-induced neuronal damage in the retina. Nitric oxide (NO) is one of the most widespread intercellular messengers in the retina (13). NO synthase (NOS) is the enzyme responsible for catalyzing the oxidation of L-arginine, yielding equimolar amounts of NO and L-citrulline. There are two constitutive Ca²⁺-dependent isoforms of NOS, endothelial (eNOS) and neuronal (nNOS), and one inducible isoform (iNOS) that is Ca²⁺ independent. nNOS and iNOS expression and activity have been described in the retina, spinal cord, and brain of mammals (11, 45, 46, 63). PA results in high levels of NO, accompanied by alterations in NOS expression and activity (11, 28, 45). NOS immunolocalization in the retina has been confirmed in amacrine, horizontal cells, ganglion cells, Müller cells, photoreceptors, and nerve fibers in the inner and outer plexiform layers of the retina (45, 59). NO reacts with the free radical superoxide exacerbating neurodegenerative processes through the forma-

* M. Rey-Funes and I. M Larrayoz contributed equally to this work.

Address for reprint requests and other correspondence: I. M. Larrayoz, Angiogenesis Study Group, Center for Biomedical Research of La Rioja (CIBIR), 26006 Logroño, Spain (e-mail: ilarrayoz@riojasalud.es).

tion of peroxynitrites, which promote protein nitration (47). In consequence, an increase in NO concentration in the retina induces cytotoxic effects (8), and NO is postulated as a key neurotoxic factor in ROP (38). Therefore inhibition of NO actions may provide therapeutic opportunities.

Methylene blue (MB) is a soluble guanylyl cyclase inhibitor that was approved by the U.S. Food and Drug Administration as an antidote for the treatment of poison-induced methemoglobinemia because of its powerful antioxidant properties (58). Soluble guanylyl cyclase is regarded as the key enzyme in mediating NO-induced effects (22, 35). It was shown that MB inhibits NADPH oxidase and myeloperoxidase enzymes (19), by either competing for oxygen (3) or acting as a free radical scavenger. Coadministration of MB and rotenone was able to prevent changes in mouse visual function and retinal histopathology (48, 62).

One of the common findings in PA specimens is the induction of angiogenesis in the inner layers of the retina. Aberrant regulation of pro- and anti-angiogenic factors under ischemic conditions may be responsible for retinal neovascularization (10). Activation of hypoxia inducible factor (HIF-1) induces NOS transcription and expression of proangiogenic factors such as adrenomedullin (AM) and vascular endothelial growth factor (VEGF). AM is involved in the induction of vasodilatation, regulation of cell proliferation, and angiogenesis (30). Under low-oxygen conditions, transactivation of the AM promoter occurs through a HIF-1 α -mediated mechanism (16). In the brain, AM is secreted by neurons and glia (51), while we have recently described AM expression in the rat retina (43).

Increased levels of VEGF have been identified in models of retinal ischemia by us and others (21, 43). Hypoxia induces significant increases in VEGF expression in cells of the ganglion cell layer of the inner retina, and this increment would promote angiogenesis (43). VEGF is able to induce expression of matrix metalloproteinases type 2 (MMP2) and type 9 (MMP9), which correlates with the progression of neovascular diseases (18). MMP expression, induced by hypoxia, down-regulates the action of the anti-angiogenic molecule, pigment epithelium-derived factor (PEDF), which is a cleavage substrate for MMPs (37). PEDF is the main anti-angiogenic and neurotrophic protein of the eye (10, 55).

The aim of the present work was to analyze the application of MB as a potential therapeutic strategy to prevent morphological and biochemical consequences of IPR in a rat model.

MATERIALS AND METHODS

Hypoxic-ischemic injury animal model. Severe perinatal asphyxia was induced using a noninvasive model of hypoxia-ischemia as described (29). Sprague-Dawley albino rats with genetic quality and sanitary certification from the animal facility of our institution were cared for in accordance with the guidelines published in the Association for Research in Vision and Ophthalmology Statement for the Use of Animals in Ophthalmic and Vision Research and in the NIH "Guide for the Care and Use of Laboratory Animals" (National Institutes of Health Publication No. 85-23, revised 1985, available from Office of Science and Health Reports, National Center for Research Resources, Bethesda, MD 20892) and the principles presented in the "Guidelines for the Use of Animals in Neuroscience Research" by the Society for Neuroscience (available from the Society for Neuroscience, Washington, DC; published in Membership Directory of the Society, pp. xxvii–xxviii, 1992). The animal model described below was approved in all its parts by the Ethical Commit-

tee of CICUAL: "Comité Institucional para el Uso y Cuidado de Animales de Laboratorio" (Resolution no. 2079/07), Facultad de Medicina, Universidad de Buenos Aires, Argentina. Appropriate proceedings were performed to minimize the number of animals used and their suffering, pain, and discomfort. Animals were kept under standard laboratory conditions at 24°C, with light-dark cycles of 12:12 h, and food and water were given ad libitum. Fifteen timed-pregnant Sprague-Dawley rats were used. The first group consisted of normally delivered, nonmanipulated pups that were used as normal controls (CTL, $n = 28$ pups). In the second group, dams were intraperitoneal injected, 30 and 5 min before euthanization, with saline solution (PA, $n = 28$ pups). The third group was intraperitoneal injected with 2 mg/kg methylene blue (Sigma, St. Louis, MO) at the same times (MB-PA, $n = 28$ pups). A fourth group consisted of MB-treated pups that were not subjected to PA (MB-CTL, $n = 14$ pups). Pregnant rats at term were euthanized by decapitation and immediately hysterectomized. All full-term fetuses, still inside the uterus, were subjected to asphyxia by transient immersion of both uterine horns in a water bath for 20 min at 37°C. After asphyxia, the uterine horns were opened, pups were removed, dried of delivery fluids, and stimulated to breathe, and their umbilical cords were ligated. The pups were then placed for recovery under a heating lamp and given to a surrogate mother. Time of asphyxia was measured as the time elapsed from the hysterectomy up to the recovery from the water bath. The overall mortality rate for the PA group was 60%, similar to previous reports (29), whereas for the MB-PA group, mortality was only 20%. To avoid the possible influence of hormonal variations due to the female estrous cycle, only male pups were included in this study.

Morphological study. Thirty-day-old CTL, PA, and MB-PA rats ($n = 4$ per group) were deeply anesthetized by an intraperitoneal injection of 300 mg/kg ketamine (Imalgene; Merial Laboratorios, Barcelona, Spain) + 30 mg/kg xylazine (Xilagesic; Proyma Ganadera, Ciudad Real, Spain) and intracardially perfused with 4% paraformaldehyde in PBS. The eyes were postfixed in the same fixative for 24 h at 4°C, cryoprotected with 20% sucrose in PBS, embedded in optimal cutting temperature compound, and sectioned in a cryostat (Leica Biosystems, Germany). Frozen sections (15 μ m thick) were stained with a monoclonal antibody against glial fibrillary acidic protein (1:500, Sigma) overnight at 4°C, exposed to a secondary antibody (1:300, FITC-anti-mouse; Vector Laboratories, Burlingame, CA), and counterstained with 4',6-diamidino-2-phenylindole (DAPI; 1:1,000, Sigma). Images were acquired in a confocal microscope (TCS SP5; Leica). Other sections were stained with biotinylated *Lycopersicon esculentum* (tomato) lectin (1:150, Sigma) and revealed with an avidin-biotin complex (ABC) kit (Vector Laboratories) followed by diaminobenzidine-nickel. Slides were counterstained with cresyl violet. To quantify the number of blood vessels, two antero-posterior sections intersecting the central area of the sagittal plane were chosen for each retina. Tomato lectin-positive vessels present in the inner layer of the retina were counted in 4/6 areas, each 400 μ m in length.

Constitutive NOS activity. Additional 30-day-old animals from the same three experimental groups ($n = 4$ per group) were similarly anaesthetized with ketamine/xylazine, euthanized by decapitation, and enucleated. Anterior segments of the eyes, including the lens, were discarded, and the retinas were dissected from the posterior segment, frozen, and stored at -80°C until used. The biochemical activity of nNOS was determined measuring the conversion of L-[U- ^{14}C]arginine into L-[U- ^{14}C]citrulline as described (41). Briefly, tissues were homogenized (1:3 wt/vol) at 4°C in homogenization buffer [20 mM HEPES, 0.2 M sucrose, 5 mM DTT, 1 mM ethylenediaminetetraacetic acid (EDTA), 10 μ g/ml soybean trypsin, 10 μ g/ml leupeptin, 2 μ g/ml pepstatin, and 0.1 mM PMSF, pH 7.4]. Homogenates were sonicated and centrifuged for 30 min at 15,000 rpm (4°C), and supernatants were collected. Protein concentration was determined by the Bradford method, using bovine serum albumin as standard. Supernatant aliquots were incubated for 20 min, at 37°C, with 20 μ M L-[U-

Table 1. Primers used for qRT-PCR in this study

Target Gene	Forward Primer	Reverse Primer
nNOS	GACAACGTTTCCTGTGGTCCT	TCCAGTGTGCTCTTTCAGGTG
iNOS	AGGCCACCTCGGATATCTCT	GCTTGTCTCTGGGTCCTCTG
MMP2	ACCGTCGCCCATCATCAA	CCTTCAGCACAAAGAGGTTGC
MMP9	TGTCCAGACCAAGGGTACAGC	GAAGAATGATCTAAGCCCAGCG
VEGF	GCCAGCACATAGGAGATGAGC	CAAGGCTCACAGTGATTTTCTGG
PEDF	ACCCTCGCATAGACCTTCAG	GGCATTTCCTTGTAGACCG
AM	CAAGCAGAGCACGTCTAGCA	GGTGAGCCAGTTTCTGCATT
GFAP	GAAGAAAACCCGATCACCAT	GGCACACCTCACATCACATC
18S	ATGCTCTTAGCTGAGTGTCCCG	ATTCCTAGCTGCGGTATCCAGG

Annealing temperature was 60°C for all primers. 18S was used as a housekeeping gene.

^{14}C arginine in incubation buffer (50 mM KH_2PO_4 , 0.2 mM CaCl_2 , 50 mM L-valine, 1 mM L-citrulline, 1.5 mM DTT, and 1 mM MgCl_2 , pH 7.4 with KOH 2 N, plus 0.75 $\mu\text{g}/\text{ml}$ NADPH, 2.15 $\mu\text{g}/\text{ml}$ FMN, 3.74 $\mu\text{g}/\text{ml}$ FAD, and 1.412 $\mu\text{g}/\text{ml}$ tetrahydrobiopterin). The reaction was stopped with addition of Dowex-50 WX8-400 ionic interchange resin, and the resultant supernatant containing L-[U- ^{14}C]citrulline was quantified. To determine the activity of nNOS, the difference between the amount of [^{14}C]citrulline produced in control samples and that in the samples processed in incubation buffer containing 2 mM ethylene

glycol-bis(β -aminoethyl ester)-*N,N,N',N'*-tetraacetic acid (EGTA) was calculated.

NADPH-diaphorase histochemistry. After anesthesia, CTL, PA, and MB-PA rats of 30 days of age ($n = 4$ per group) were intracardially perfused with physiological solution followed by 4% paraformaldehyde in 0.1 M pH 7.4 phosphate buffer at 4°C. The posterior segments of the eyes containing the retinas were postfixed overnight in the same fixative at 4°C. Following cryoprotection with increasing sucrose concentrations (10, 20, and 30%) in phosphate buffer saline at 4°C overnight, tissues were included in Tissue Teck, frozen in powdered dry ice, and stored at -80°C . Sections (15 μm thick) were obtained using a Leitz "Lauda" cryostat and mounted onto gelatin-coated slides (2.5% gelatine, 1% Elmer's glue), air dried at room temperature, and stored at -80°C until their use. Cryostat sections (thickness 18 μm) were mounted onto gelatin-coated slides and incubated with 0.1% β -NADPH (Sigma) and 0.02% nitroblue tetrazolium (Sigma) diluted in 0.1 M phosphate buffer (PB), pH 7.4, with 1% Triton X-100, for 1 h at 37°C. As a negative control, β -NADPH was omitted in adjacent sections. NADPH-diaphorase reactivity was detected as a blue precipitate. Then, sections were washed in PB, dehydrated in an alcohol series, quickly cleared with xylol, and coverslipped.

NOS immunohistochemistry. For immunohistochemical detection of neuronal NOS (nNOS), slides were obtained as above, and endogenous peroxidase activity was blocked with 1% hydrogen peroxide in

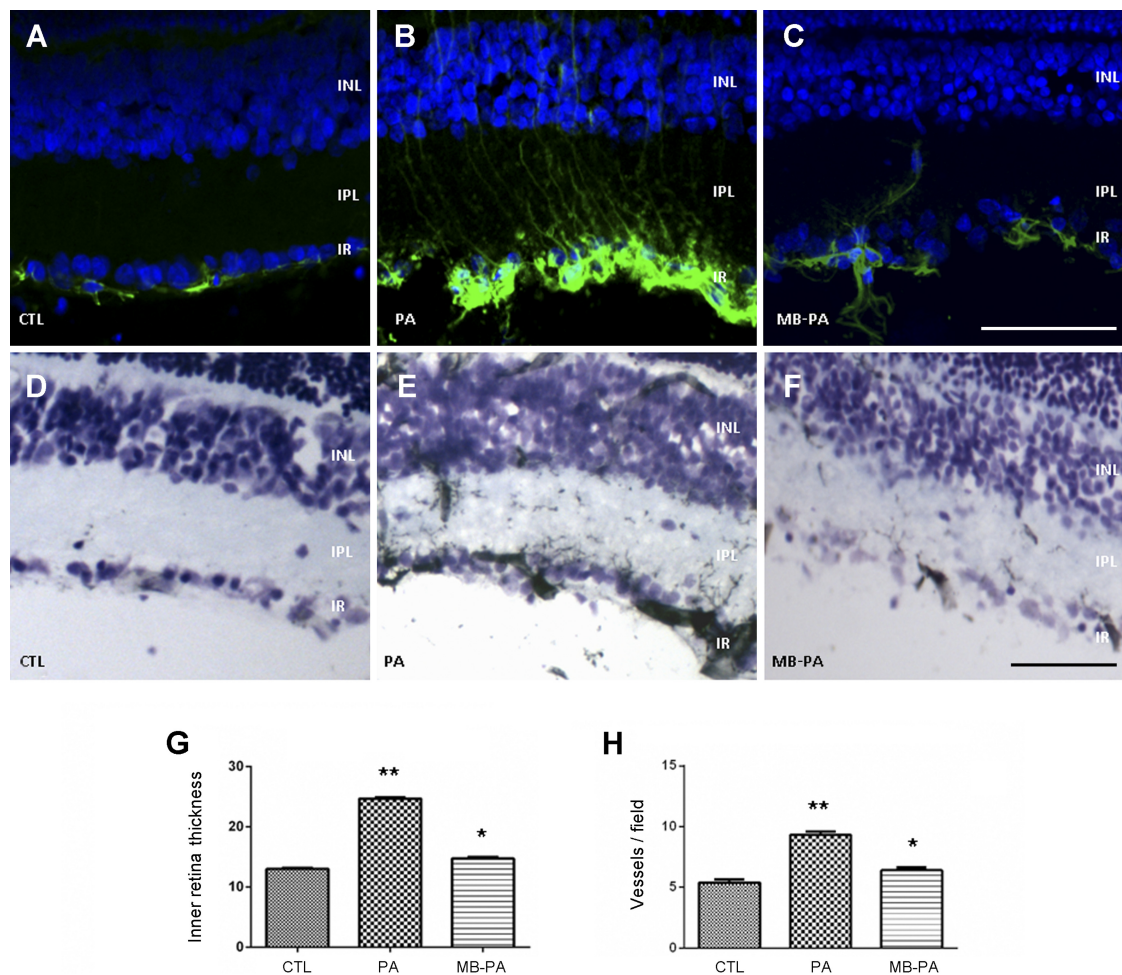


Fig. 1. Representative micrographs of the inner retina in rats of the experimental groups CTL (A, D), PA (B, E), and MB (C, F) immunostained with an antibody against GFAP (green, A–C) or with tomato lectin (D–F). Using these sections, the thickness of the inner retina (G) and the number of blood vessels per microscopic field (H) were quantified. INL, inner nuclear layer; IPL, inner plexiform layer; IR, inner retina. Size bar = 50 μm . Bars represent the mean \pm SD of all measurements ($n = 4$ animals, 6 sections per animal). The asterisks represent statistically significant differences with the CTL group. * $P < 0.05$; ** $P < 0.01$.

PB for 30 min. Then, sections were blocked with 10% normal goat serum in PBS, pH 7.4, for 1 h. Slides were incubated overnight (at 4°C) with a rabbit polyclonal anti-nNOS antibody (1:3,000 dilution) produced at the Cajal Institute (46). The specificity of the staining was corroborated in adjacent sections by omission of the primary antibody. Immunoreactivity was visualized with biotinylated goat anti-rabbit IgG (1:100; Sigma), developed with the ABC kit (Vector Laboratories) and 0.03% 3,3'-diaminobenzidine (Sigma), 3% nickel ammonium sulphate, and 0.01% hydrogen peroxide diluted in 0.1 M buffer acetate, yielding a black product. Sections were dehydrated, cleared, and mounted.

SDS-PAGE and Western blotting. Retinas of 30-day-old rats of the three groups were dissected out ($n = 4$ per experimental group). Tissues were homogenized (1:3, wt/vol) in lysis buffer (see above) at 4°C. Homogenates were centrifuged for 30 min at 15,000 g, and the supernatants were collected. Protein concentration was determined by the Bradford method, with bovine serum albumin as standard, using a NanoDrop spectrophotometer (ND100). Then, 25 μ g of each sample were mixed 1:1 with sample buffer [10 ml Tris-HCl 0.5 M, pH 6.8, 16 ml sodium dodecylsulphate (SDS) 10% (wt/vol), 8 ml glycerol, 2 ml 2-mercaptoethanol, and 0.2 ml bromophenol blue 0.1% (wt/vol)] and heated for 3 min at 95°C. Samples were run on SDS-polyacrylamide gels (10% running gel with 3.5% stacking gel), with 0.25 M Tris-glycine, pH 8.3, as the electrolyte buffer, in a Bio-Rad Mini-Protein II (Bio-Rad, Madrid, Spain). Kaleidoscope Prestained Standards (Bio-Rad) were used as molecular weight markers. For Western blot analysis, proteins were transferred at 1.5 mA/cm² for 1 h onto 0.2- μ m polyvinylidene difluoride membranes (Immobilon-P; Millipore, Bedford, MA) by semi-dry transfer methods (Bio-Rad). For protein identification, membranes were incubated overnight at 4°C with primary antibodies (rabbit anti-nNOS at 1:1,000; rabbit anti-MMP2 from Abbiotec at 1:500; mouse anti-MMP9 from Millipore at 1:500; or rabbit anti-PEDF from Bioproducts MD at 1:500). To standardize the results, a monoclonal IgG anti- β -actin antibody (Abcam) was used at a dilution 1:5,000 in the same membranes. To visualize immunoreactivity, membranes were incubated with anti-rabbit or anti-mouse peroxidase-labeled IgGs, developed with a chemoluminescence kit (GE Biosciences, Miami, FL), and exposed to X-ray blue films (CEA, Strängnäs, Sweden). Developed films were scanned with a computer-assisted densitometer (GS-800; Bio-Rad), and optical density was quantified by NIH Scion Image software.

Zymograms. Retinas from 24-h-old animals of the CTL, PA, and MB-PA groups ($n = 4$ per group) were homogenized in lysis buffer, and total protein contents were quantified as above. Equal amounts of protein (50 μ g) were loaded on each well of a 10% gelatin zymogram gel (Invitrogen, Carlsbad, CA). After electrophoresis, the gel was incubated for 30 min in renaturing buffer and then in developing buffer for another 30 min, both at room temperature. Gels were incubated in developing buffer overnight at 37°C. Following several washes, the gels were stained with Simply Blue (Invitrogen), destained, and scanned with Odyssey (Li-cor, Lincoln, NE). Gelatinolytic activity for each enzyme (MMP2, 72 kDa; MMP9, 92 kDa) was quantified by image analysis (Image-J; NIH, Bethesda, MD).

Image analysis. Six random retinal sections from four animals of each experimental group were analyzed. Care was taken on selecting anatomically matched areas of retina among animals before assays. Slides were analyzed using an Olympus BH2 microscope (Olympus Optical, Tokyo, Japan) attached to a video camera (CCD Sony-XC77) coupled to a computer equipped with a video card (Data Translation). The central area of the sagittal plane was chosen for each retina. Inner retina thickness, relative optical density (R.O.D.), immunoreactive cellular area (I.C.A.), and number of immunoreactive cells per surface unit were evaluated using the Scion Image software (developed by W. Rasband, 1995, NIH, Research Services Branch, National Institute of Mental Health, Bethesda, MD). Only those cells that had a grey level darker than a defined "threshold" (defined as the optic density three-fold higher than the mean background density) were considered

specific immunoreactively stained cells. The mean background density was measured in a region devoid of immunoreactive cells, immediately adjacent to the analyzed region. R.O.D. was calculated using a gray scale of 255 gray levels. To avoid external variations, all images were taken the same day and under the same light conditions. The number of cells was measured in retina segments of exactly 160 μ m in length. Four segments were measured in each retinal section. Since immunohistochemistry and Western blotting are semiquantitative techniques, R.O.D. values were expressed as percentage of change with respect to the CTL group considering CTL's R.O.D. as 100%. Colocalization was studied by immunofluorescence using a Nikon C1 Plus laser microscope (Nikon Inverted Research Microscope Eclipse Ti; Nikon, Tokyo, Japan), and images were analyzed with the EZ-C1 software (EZ-C1 Software v3.9; Nikon). Adobe Photoshop software (Adobe Photoshop CS5; Adobe Systems, Ottawa, Ontario, Canada) was used for digital manipulation of only brightness and contrast when preparing the shown images.

RNA isolation and quantitative real-time polymerase chain reaction (qRT-PCR). At different times (2, 6, 12, 24, and 48 h) after recovery from asphyxia, pups of the three experimental groups (CTL, PA, and MB-PA) ($n = 4$ per group) were deeply anesthetized with ketamine-xylazine, decapitated, and enucleated. The posterior segments of the eyes were frozen and stored at -80°C until used. Tissues were homogenized with TRIzol (Invitrogen, Madrid, Spain), and RNA was isolated with RNeasy Mini kit (Qiagen, Germantown, MD). Three micrograms of total RNA was treated with 0.5 μ l DNaseI

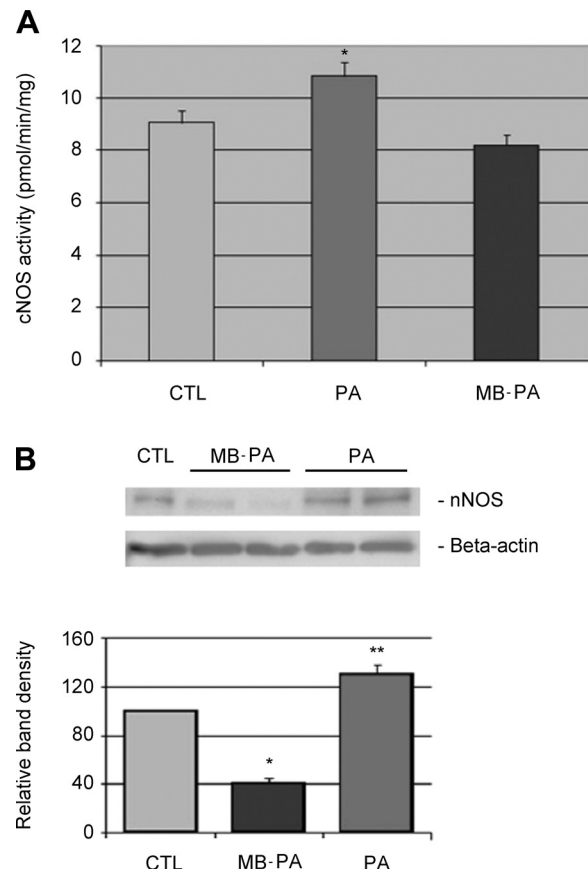


Fig. 2. Enzymatic activity for constitutive NOS (A) and Western blot analysis for nNOS (B) in the retina of control animals (CTL), rats subjected to perinatal asphyxia (PA), and animals treated with methylene blue before the asphyxia (MB-PA). Western blots were quantified by densitometry, and the nNOS values were normalized by β -actin. Each bar represents the mean \pm SD of all measurements ($n = 4$). The asterisks represent statistically significant differences with the CTL group. * $P < 0.05$; ** $P < 0.01$.

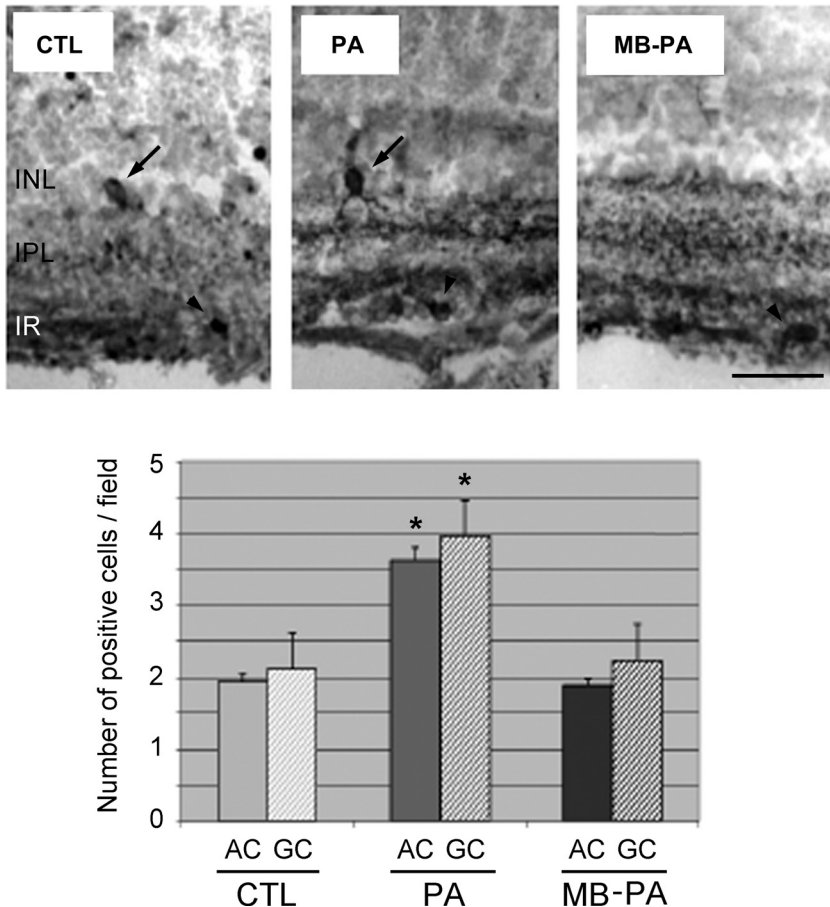


Fig. 3. Immunohistochemical staining for nNOS in the retina of control animals (CTL), rats subjected to perinatal asphyxia (PA), and animals treated with methylene blue before the asphyxia (MB). Amacrine (arrows) and ganglion (arrowheads) cells are immunoreactive for nNOS. INL, inner nuclear layer; IPL, inner plexiform layer; IR, inner retina. Size bar = 25 μ m. The number of nNOS-positive amacrine cells (AC) and ganglion cells (GC) per field was quantified and is represented in a histogram. Each bar represents the mean \pm SD of all measurements ($n = 4$ animals, 6 sections per animal). The asterisks represent statistically significant differences with the CTL group. * $P < 0.05$.

(Invitrogen) and reverse-transcribed into first-strand cDNA using random primers and the SuperScript III kit (Invitrogen). Reverse transcriptase was omitted in control reactions, where the absence of PCR-amplified DNA confirmed lack of contamination from genomic DNA. Resulting cDNA was mixed with SYBR Green PCR Master Mix (Invitrogen) for quantitative real-time polymerase chain reaction (qRT-PCR) using 0.3 μ M forward and reverse oligonucleotide primers (Table 1). Quantitative measures were performed using a 7300 Real Time PCR System (Applied Biosystems, Carlsbad, CA). Cycling conditions were an initial denaturation at 95°C for 10 min, followed by 40 cycles of 95°C for 15 s and 60°C for 1 min. At the end, a dissociation curve was implemented from 60 to 95°C to validate amplicon specificity. Gene expression was calculated using absolute quantification by interpolation into a standard curve. All values were divided by the expression of the housekeeping gene 18S.

Statistical analysis. Values are expressed as means \pm SD. At least two experimental repeats were evaluated in all cases. Twelve sections of each animal were analyzed. Results were evaluated using one-way analysis of variance (ANOVA), and comparisons between groups were made by Fisher, Scheffé, and Bonferroni-Dunn tests, using GraphPad software (GraphPad Software, San Diego, CA). Differences were considered significant when $P < 0.05$.

RESULTS

MB reduces asphyxia-induced inner retinal thickness, gliosis, and angiogenesis. Perinatal asphyxia induced an increase in inner retinal thickness (Fig. 1, A, B, and G), gliosis as revealed by GFAP staining (Fig. 1, A and B), and retinal angiogenesis as shown by tomato lectin staining (Fig. 1, D, E,

and H) when compared with nonasphyxiated control animals. Application of MB significantly reduced the increase in all these parameters (Fig. 1, C and F–H).

nNOS isoform expression and activity are modulated by MB in adult rats. First, we investigated whether MB had any influence on regulating asphyxia-induced increased NOS activity. As previously shown (43), the retinas of animals subjected to perinatal asphyxia had higher constitutive NOS enzymatic activity than control animals (Fig. 2A). Similar results were obtained when studying nNOS protein expression in Western blots. The retina of asphyctic animals had higher levels of nNOS than control rats ($P < 0.01$), but the treatment with MB reduced constitutive NOS activity and

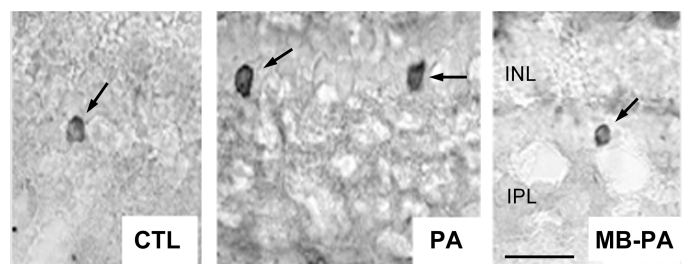


Fig. 4. Histochemical staining for NADPH-diaphorase (arrows) in the retina of control animals (CTL), rats subjected to perinatal asphyxia (PA), and animals treated with methylene blue before the asphyxia (MB-PA). INL, inner nuclear layer; IPL, inner plexiform layer. Size bar = 25 μ m. Quantification of these data appears in Table 2.

Table 2. Morphometric parameters of NADPH-diaphorase-positive amacrine cells

Treatment	Number of Cells per Field	Cellular Area, μm^2	Cellular Area (R.O.D.)	Immunoreactive Cellular Area, μm^2	Immunoreactive Cellular Area (R.O.D.)
CTL	2.00 \pm 0.20	84.52 \pm 2.02	0.45 \pm 0.16	54.01 \pm 2.35	0.48 \pm 0.07
PA	3.07 \pm 0.18*	95.14 \pm 1.52*	0.60 \pm 0.05*	68.68 \pm 1.89*	0.63 \pm 0.04*
MB-PA	1.49 \pm 0.16*	89.14 \pm 2.71	0.48 \pm 0.13	55.22 \pm 3.48	0.49 \pm 0.36

R.O.D., relative optical density. Asterisks represent statistically significant differences with CTL. * $P < 0.05$.

nNOS expression even below control levels (Fig. 2, A and B).

A morphometric analysis was carried out studying both nNOS immunoreactivity and NADPH-diaphorase reactivity (an enzymatic activity of the NOS enzymes). In both cases, some ganglion cells and some amacrine cells stained positive (Figs. 3 and 4). The number of nNOS immunoreactive cells was significantly higher in the PA group for both cell types, and MB prevented this increase in all cases (Fig. 3). The same pattern was observed with the NADPH-diaphorase staining (Fig. 4), which is quantified in Table 2.

Expression of angiogenesis-regulating factors. The expression of several key regulators was studied over time. These included nNOS, iNOS, GFAP, the proangiogenic factors VEGF and AM, MMP2, MMP9, and the anti-angiogenic factor PEDF. No changes were found in the expression of nNOS, iNOS, or GFAP, suggesting that the regulation of these gene products is posttranscriptional. Contrary to expectation, PA did not induce overexpression of VEGF or AM at any of the times tested (not shown). At the transcriptional level, there was a significant increase in MMP2 expression elicited by MB treatment at 6-h postasphyxia (Fig. 5A), but MMP2 gelatinolytic

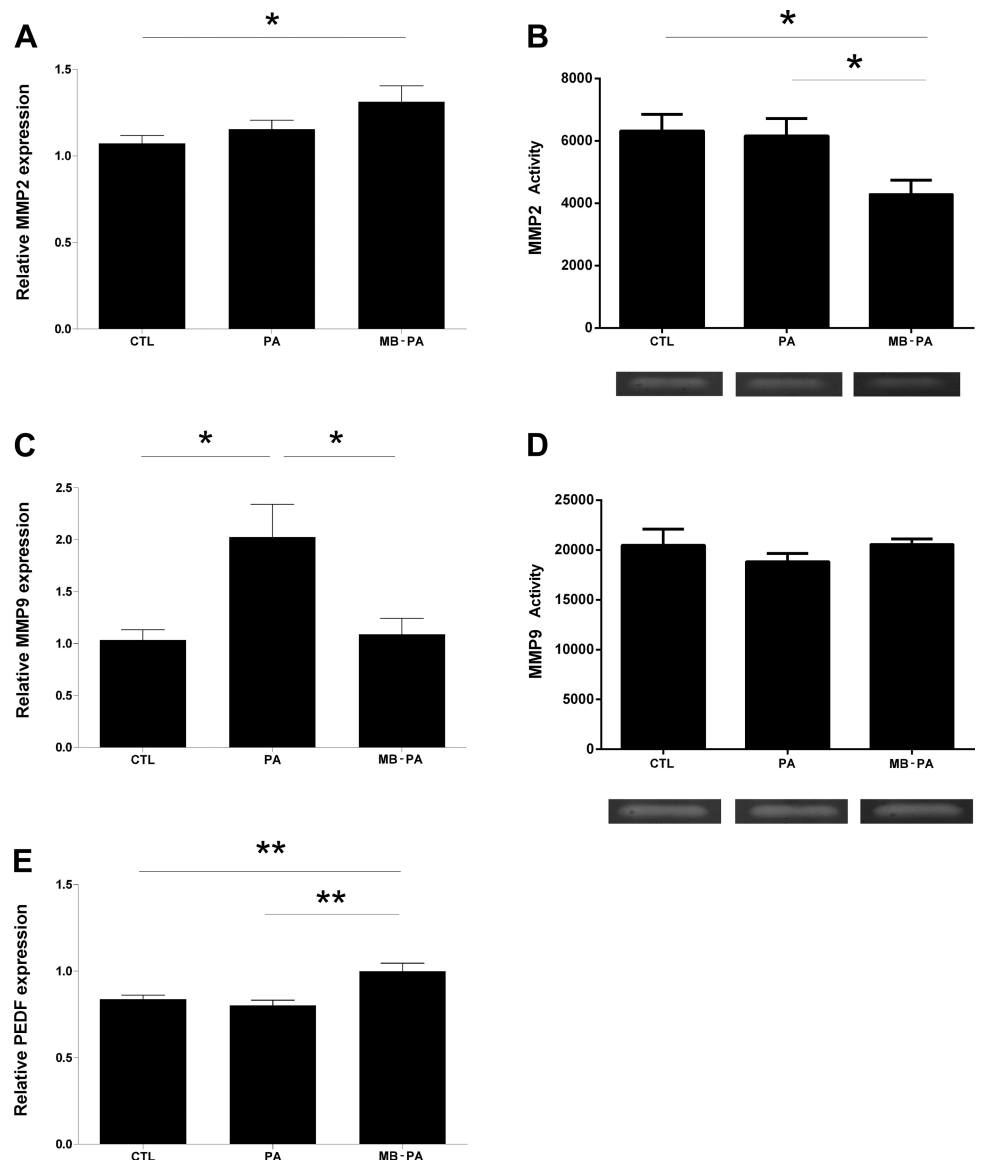


Fig. 5. Quantitative real-time PCR analysis of the expression of MMP2 (A), MMP9 (C), and PEDF (E) and zymograms for MMP2 (B) and MMP9 (D) in the three experimental groups. All gene data were referenced to the value of the housekeeping gene 18S in the same sample. Primer sequences can be found in Table 1. Each bar represents the mean \pm SD of all measurements ($n = 4$). The asterisks represent statistically significant differences as indicated. * $P < 0.05$; ** $P < 0.01$.

activity significantly decreased 2 h after asphyxia (Fig. 5B). MMP9 mRNA expression showed a marked increase in asphyctic animals at 6 h, and this was significantly attenuated by MB (Fig. 5C). No changes were observed in gelatinolytic activity for MMP9 at 2 h (Fig. 5D). When MMP expression was investigated by Western blotting, no significant changes were observed for either MMP2 or MMP9 (Fig. 6, A and B). Interestingly, the anti-angiogenic factor PEDF did not change by asphyxia but had a significant upregulation following MB treatment (Fig. 5E). This result was further confirmed by Western blotting (Fig. 6C).

DISCUSSION

This work demonstrates that MB is an effective agent against a number of the deleterious effects of perinatal asphyxia in the retina; these benefits were accompanied by changes in NO, MMPs, and PEDF. Therefore MB could be useful in reducing IPR development. Previously, we showed that NO increases in the retina 21 days after injury (45). Here we determined that application of MB inhibited NOS enzymatic activity, thus blocking the NO-dependent neurotoxic cascade.

The most sensitive region of the eye to oxygen shortage corresponds to the innermost layers of the retina (38). In this region, we identified enhanced expression of nNOS in amacrine and ganglion cells following experimental asphyxia (45). Excessive production of NO could be highly toxic, combining with other reactive oxygen species to form peroxynitrite and destroying vital cell components (47). Here we have shown that MB can stop the whole cascade of events by preventing excessive NO formation.

Experimental therapeutic strategies against ROP described in the literature include the use of antioxidants (42), D-penicillamine (40), allopurinol (50), indomethacin (36), dexamethasone (49), rofecoxib (57), and angiotensin-system modulators (12), among others. However, the most effective treatment to prevent retinopathy, so far, is hypothermia. A therapeutic trial employing hypothermia showed a significant decrease in brain tissue injury, and improved survival and neurological outcomes, at up to 18 mo of age (4). Recently, we have reported that hypothermia is able to prevent gliosis and angiogenesis development in an experimental model of IPR (43). While both hypothermia and MB are effective in protecting the retina, the latter agent acts directly on the nitrergic system, competing with NO for binding to iron in soluble guanylate (34), preventing the increase of cyclic GMP and its negative effects as shown in cardiac and pulmonary tissues (2, 32, 60). NO is also related to angiogenesis by increasing survival of endothelial cells (64) and by being downstream of the VEGF signaling pathway (54). In addition, NO regulates MMP9 expression (31).

In our qRT-PCR data we found no changes in the expression of nNOS, iNOS, or GFAP despite the fact that physiological changes were observed through NOS activity measurements or by immunostaining for GFAP. These apparent discrepancies can be explained by the time at which the mRNA was collected (from 2 to 48 h) and the time at which activity and immunohistochemistry were measured (30 days). A surprising observation was that the proangiogenic factors VEGF and AM did not show any upregulation in the PA group, despite the fact that both molecules are regulated by hypoxia and HIF-1 α (16, 25). This may indicate that these factors do not play a relevant role in regulating PA-induced angiogenesis at these times. In previous studies, AM was elevated 7-days posthypoxia and VEGF was elevated 15-days posthypoxia (43). In this context, the molecules that may also be regulating angiogenesis are the MMPs and PEDF. MMP2 was not affected by PA, but we observed an initial downregulation of its gelatinolytic activity by MB at 2 h, followed by a mRNA upregulation at 6 h. For MMP9 we saw no change at 2 h but a clear mRNA overexpression in the PA group at 6 h, which was significantly reduced in the MB group. There were no significant changes in

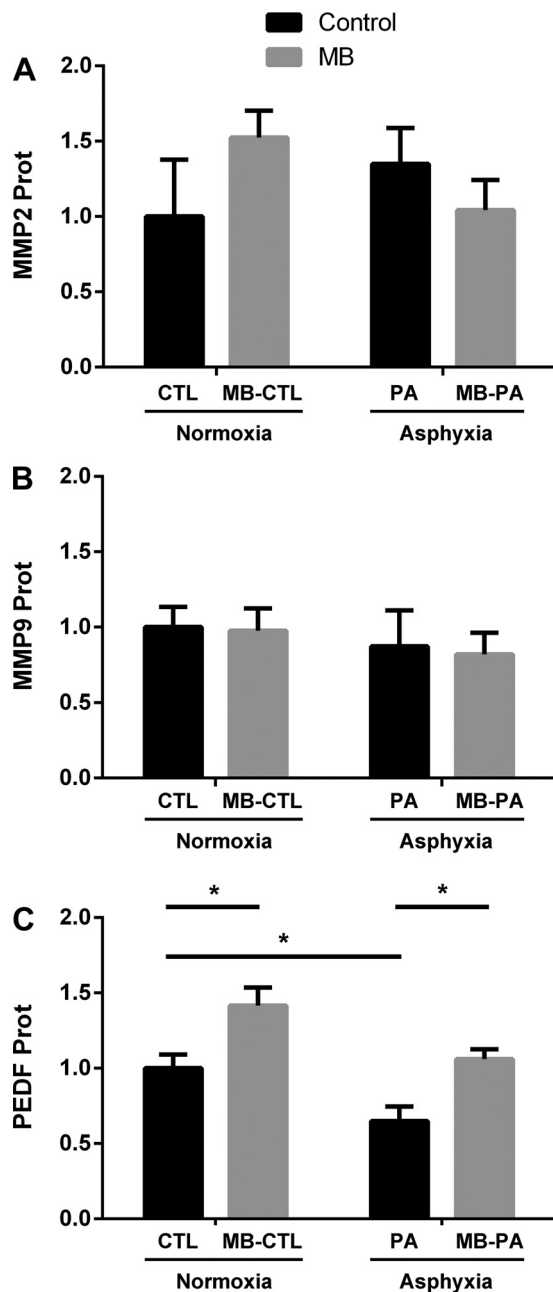


Fig. 6. Western blotting for MMP2 (A), MMP9 (B), and PEDF (C) was performed in retinas of the four experimental groups at 6 h after treatments. Each bar represents the mean \pm SD of all measurements ($n = 6$). The asterisks represent statistically significant differences as indicated. * $P < 0.05$.

MMP protein expression by Western blotting, but the regulation of these proteins is complex and involves several other proteins such as TIMPs, among others. Thus we believe that the most relevant results are those obtained by zymography since they represent the quantitative gelatinolytic effects of these proteins. Both gelatinases are involved in angiogenesis (24), and the diminution of MMP2 gelatinolytic activity by MB treatment identifies this gelatinase as one of the main targets of MB in the retina. MMP2 could be responsible for the inhibition of fibrosis and angiogenesis in the inner retina of animals treated with MB. Another interesting behavior is the one protagonized by PEDF. The expression of this anti-angiogenic protein (37) did not change under asphyctic conditions, but it was significantly upregulated by MB, even in the absence of asphyxia. The activation of PEDF may explain the anti-angiogenic properties of MB since this protein is the main angiogenesis inhibitor in the eye (7) and an MMP target (32).

MB is used in the clinic for several applications, including norepinephrine-refractory hypotension (53) and the surgical management of hyperparathyroidism (5). We have to take into consideration the difficulty of applying a preventative measure at the exact time of injury in a clinical setting. Nevertheless, although formal randomized clinical trials have not been performed on this drug, its safety profile is high (5, 26), so we can envision a scenario where MB is used as a therapeutic option in cases with a high risk of developing perinatal asphyxia (6, 33).

Perspectives and Significance

MB treatment reduced retinal damage originated by perinatal asphyxia. Since this compound has been previously used in the clinic with low to no side effects, clinical trials are warranted in cases with a high risk of developing perinatal asphyxia.

ACKNOWLEDGMENTS

We thank Andrea Pecile and Manuel Antonio Ponce for excellent assistance with animal care.

DISCLOSURES

No conflicts of interest, financial or otherwise, are declared by the author(s).

AUTHOR CONTRIBUTIONS

M.R.-F., I.M.L., A.M., and C.F.L. conception and design of research; M.R.-F., I.M.L., J.C.F., D.S.C., F.R., P.I.F.I., R.M.-M., J.J.L.-C., and V.B.D. performed experiments; M.R.-F., I.M.L., J.C.F., D.S.C., F.R., P.I.F.I., R.M.-M., J.J.L.-C., and V.B.D. analyzed data; M.R.-F., I.M.L., A.M., and C.F.L. interpreted results of experiments; M.R.-F., I.M.L., and A.M. prepared figures; M.R.-F., I.M.L., A.M., and C.F.L. drafted manuscript; M.R.-F., I.M.L., A.M., and C.F.L. edited and revised manuscript; M.R.-F., I.M.L., J.C.F., D.S.C., F.R., P.I.F.I., R.M.-M., J.J.L.-C., V.B.D., A.M., and C.F.L. approved final version of manuscript.

REFERENCES

1. **American Psychiatric Association.** *Diagnosis and Statistical Manual of Mental Disorders (DSM III)*. Washington DC: American Psychiatric Association, 1987.
2. **Argenziano M, Chen JM, Choudhri AF, Cullinane S, Garfein E, Weinberg AD, Smith CR Jr, Rose EA, Landry DW, and Oz MC.** Management of vasodilatory shock after cardiac surgery: identification of predisposing factors and use of a novel pressor agent. *J Thorac Cardiovasc Surg* 116: 973–980, 1998.
3. **Atamna H, Nguyen A, Schultz C, Boyle K, Newberry J, Kato H, Ames BN.** Methylene blue delays cellular senescence and enhances key mitochondrial biochemical pathways. *FASEB J* 22: 703–712, 2008.
4. **Azzopardi D, Brocklehurst P, Edwards D, Halliday H, Levene M, Thoresen M, Whitelaw A.** The TOBY Study. Whole body hypothermia for the treatment of perinatal asphyxial encephalopathy: a randomised controlled trial. *BMC Pediatr* 8: 17, 2008.
5. **Bewick J, Pfeleiderer A.** The value and role of low dose methylene blue in the surgical management of hyperparathyroidism. *Ann R Coll Surg Engl* 96: 526–529, 2014.
6. **Bogdanovic G, Babovic A, Rizvanovic M, Ljuca D, Grgic G, Djuranovic-Milicic J.** Cardiotocography in the prognosis of perinatal outcome. *Med Arch* 68: 102–105, 2014.
7. **Bouck N.** PEDF: anti-angiogenic guardian of ocular function. *Trends Mol Med* 8: 330–334, 2002.
8. **Chemtob S, Hardy P, Abran D, Li DY, Peri K, Cuzzani O, Varma DR.** Peroxide-cyclooxygenase interactions in postasphyxial changes in retinal and choroidal hemodynamics. *J Appl Physiol* (1985) 78: 2039–2046, 1995.
9. **Chowdhury HR, Thompson S, Ali M, Alam N, Yunus M, Streatfield PK.** Causes of neonatal deaths in a rural subdistrict of Bangladesh: implications for intervention. *J Health Popul Nutr* 28: 375–382, 2010.
10. **Dawson DW, Volpert OV, Gillis P, Crawford SE, Xu H, Benedict W, Bouck NP.** Pigment epithelium-derived factor: a potent inhibitor of angiogenesis. *Science* 285: 245–248, 1999.
11. **Dorfman VB, Rey-Funes M, Bayona JC, Lopez EM, Coirini H, Loidl CF.** Nitric oxide system alteration at spinal cord as a result of perinatal asphyxia is involved in behavioral disabilities: hypothermia as preventive treatment. *J Neurosci Res* 87: 1260–1269, 2009.
12. **Downie LE, Pianta MJ, Vingrys AJ, Wilkinson-Berka JL, Fletcher EL.** AT1 receptor inhibition prevents astrocyte degeneration and restores vascular growth in oxygen-induced retinopathy. *Glia* 56: 1076–1090, 2008.
13. **Eldred WD, Blute TA.** Imaging of nitric oxide in the retina. *Vision Res* 45: 3469–3486, 2005.
14. **Ferriero DM.** Neonatal brain injury. *N Engl J Med* 351: 1985–1995, 2004.
15. **Fottrell E, Osrin D, Alcock G, Azad K, Bapat U, Beard J, Bondo A, Colbourn T, Das S, King C, Manandhar D, Manandhar S, Morrison J, Mwansambo C, Nair N, Nambiar B, Neuman M, Phiri T, Saville N, Sen A, Seward N, Shah MN, Shrestha BP, Singini B, Tumbahangphe KM, Costello A, Prost A.** Cause-specific neonatal mortality: analysis of 3772 neonatal deaths in Nepal, Bangladesh, Malawi and India. *Arch Dis Child Fetal Neonatal Ed* 100: F439–F447, 2015.
16. **Garayoa M, Martinez A, Lee S, Pio R, An WG, Neckers L, Trepel J, Montuenga LM, Ryan H, Johnson R, Gassmann M, Cuttitta F.** Hypoxia-inducible factor-1 (HIF-1) up-regulates adrenomedullin expression in human tumor cell lines during oxygen deprivation: a possible promotion mechanism of carcinogenesis. *Mol Endocrinol* 14: 848–862, 2000.
17. **Grow J, Barks JD.** Pathogenesis of hypoxic-ischemic cerebral injury in the term infant: current concepts. *Clin Perinatol* 29: 585–602, 2002.
18. **Heo SH, Choi YJ, Ryoo HM, Cho JY.** Expression profiling of ETS and MMP factors in VEGF-activated endothelial cells: role of MMP-10 in VEGF-induced angiogenesis. *J Cell Physiol* 224: 734–742, 2010.
19. **Heydrick SJ, Reed KL, Cohen PA, Aarons CB, Gower AC, Becker JM, Stuechi AF.** Intraperitoneal administration of methylene blue attenuates oxidative stress, increases peritoneal fibrinolysis, and inhibits intra-abdominal adhesion formation. *J Surg Res* 143: 311–319, 2007.
20. **Hill A.** Current concepts of hypoxic-ischemic cerebral injury in the term newborn. *Pediatr Neurol* 7: 317–325, 1991.
21. **Hofman P, van Blijswijk BC, Gaillard PJ, Vrensen GF, Schlingemann RO.** Endothelial cell hypertrophy induced by vascular endothelial growth factor in the retina: new insights into the pathogenesis of capillary nonperfusion. *Arch Ophthalmol* 119: 861–866, 2001.
22. **Hwang TL, Wu CC, Teng CM.** Comparison of two soluble guanylyl cyclase inhibitors, methylene blue and ODQ, on sodium nitroprusside-induced relaxation in guinea-pig trachea. *Br J Pharmacol* 125: 1158–1163, 1998.
23. **Kalter HD, Roubanatou AM, Koffi A, Black RE.** Direct estimates of national neonatal and child cause-specific mortality proportions in Niger by expert algorithm and physician-coded analysis of verbal autopsy interviews. *J Glob Health* 5: 010415, 2015.

24. Kowluru RA, Zhong Q, Santos JM. Matrix metalloproteinases in diabetic retinopathy: potential role of MMP-9. *Expert Opin Investig Drugs* 21: 797–805, 2012.
25. Kurihara T, Westenskow PD, Friedlander M. Hypoxia-inducible factor (HIF)/vascular endothelial growth factor (VEGF) signaling in the retina. *Adv Exp Med Biol* 801: 275–281, 2014.
26. Landoni G, Pasin L, Di Prima AL, Dossi R, Taddeo D, Zangrillo A. Methylene blue: between Scylla (meta-analysis) and Charybdis (propensity). *J Cardiothorac Vasc Anesth* 28: e12–3, 2014.
27. Liu L, Oza S, Hogan D, Perin J, Rudan I, Lawn JE, Cousens S, Mathers C, Black RE. Global, regional, and national causes of child mortality in 2000–13, with projections to inform post-2015 priorities: an updated systematic analysis. *Lancet* 385: 430–440, 2015.
28. Loidl CF, De Vente J, van Ittersum MM, Van Dijk EH, Vles JS, Steinbusch HW, Blanco CE. Hypothermia during or after severe perinatal asphyxia prevents increase in cyclic GMP-related nitric oxide levels in the newborn rat striatum. *Brain Res* 791: 303–307, 1998.
29. Loidl CF, Gavilanes AW, Van Dijk EH, Vreuls W, Blokland A, Vles JS, Steinbusch HW, Blanco CE. Effects of hypothermia and gender on survival and behavior after perinatal asphyxia in rats. *Physiol Behav* 68: 263–269, 2000.
30. Lopez J, Martinez A. Cell and molecular biology of the multifunctional peptide, adrenomedullin. *Int Rev Cytol* 221: 1–92, 2002.
31. Manabe S, Gu Z, Lipton SA. Activation of matrix metalloproteinase-9 via neuronal nitric oxide synthase contributes to NMDA-induced retinal ganglion cell death. *Invest Ophthalmol Vis Sci* 46: 4747–4753, 2005.
32. Marczin N, Ryan US, Catravas JD. Methylene blue inhibits nitrovasodilator- and endothelium-derived relaxing factor-induced cyclic GMP accumulation in cultured pulmonary arterial smooth muscle cells via generation of superoxide anion. *J Pharmacol Exp Ther* 263: 170–179, 1992.
33. Martinez-Biarge M, Diez-Sebastian J, Wusthoff CJ, Mercuri E, Cowan FM. Antepartum and intrapartum factors preceding neonatal hypoxic-ischemic encephalopathy. *Pediatrics* 132: e952–e959, 2013.
34. Mayer B, Brunner F, Schnidt K. Novel actions of methylene blue. *Eur Heart J* 14, Suppl. 1: 22–26, 1994.
35. Nagai-Kusuhara A, Nakamura M, Mukuno H, Kanamori A, Negi A, Seigel GM. cAMP-responsive element binding protein mediates a cGMP/protein kinase G-dependent anti-apoptotic signal induced by nitric oxide in retinal neuro-glial progenitor cells. *Exp Eye Res* 84: 152–162, 2007.
36. Nandgaonkar BN, Rotschild T, Yu K, Higgins RD. Indomethacin improves oxygen-induced retinopathy in the mouse. *Pediatr Res* 46: 184–188, 1999.
37. Notari L, Miller A, Martinez A, Amaral J, Ju M, Robinson G, Smith LE, Becerra SP. Pigment epithelium-derived factor is a substrate for matrix metalloproteinase type 2 and type 9: implications for downregulation in hypoxia. *Invest Ophthalmol Vis Sci* 46: 2736–2747, 2005.
38. Osborne NN, Casson RJ, Wood JP, Chidlow G, Graham M, Melena J. Retinal ischemia: mechanisms of damage and potential therapeutic strategies. *Prog Retin Eye Res* 23: 91–147, 2004.
39. Perlman JM. Brain injury in the term infant. *Semin Perinatol* 28: 415–424, 2004.
40. Phelps DL, Lakatos L, Watts JL. D-Penicillamine for preventing retinopathy of prematurity in preterm infants. *Cochrane Database Syst Rev* 9: CD001073, 2000.
41. Radomski MW, Vallance P, Whitley G, Foxwell N, Moncada S. Platelet adhesion to human vascular endothelium is modulated by constitutive and cytokine induced nitric oxide. *Cardiovasc Res* 27: 1380–1382, 1993.
42. Raju TN, Langenberg P, Bhutani V, Quinn GE. Vitamin E prophylaxis to reduce retinopathy of prematurity: a reappraisal of published trials. *J Pediatr* 131: 844–850, 1997.
43. Rey-Funes M, Dorfman VB, Ibarra ME, Pena E, Contartese DS, Goldstein J, Acosta JM, Larrayoz IM, Martinez-Murillo R, Martinez A, Loidl CF. Hypothermia prevents gliosis and angiogenesis development in an experimental model of ischemic proliferative retinopathy. *Invest Ophthalmol Vis Sci* 54: 2836–2846, 2013.
44. Rey-Funes M, Ibarra ME, Dorfman VB, Lopez EM, Lopez-Costa JJ, Coirini H, Loidl CF. Hypothermia prevents the development of ischemic proliferative retinopathy induced by severe perinatal asphyxia. *Exp Eye Res* 90: 113–120, 2010.
45. Rey-Funes M, Ibarra ME, Dorfman VB, Serrano J, Fernandez AP, Martinez-Murillo R, Martinez A, Coirini H, Rodrigo J, Loidl CF. Hypothermia prevents nitric oxide system changes in retina induced by severe perinatal asphyxia. *J Neurosci Res* 89: 729–743, 2011.
46. Rodrigo J, Alonso D, Fernandez AP, Serrano J, Richart A, Lopez JC, Santacana M, Martinez-Murillo R, Bentura ML, Ghiglione M, Utenthal LO. Neuronal and inducible nitric oxide synthase expression and protein nitration in rat cerebellum after oxygen and glucose deprivation. *Brain Res* 909: 20–45, 2001.
47. Rodrigo J, Fernandez AP, Serrano J, Peinado MA, Martinez A. The role of free radicals in cerebral hypoxia and ischemia. *Free Radic Biol Med* 39: 26–50, 2005.
48. Rojas JC, John JM, Lee J, and Gonzalez-Lima F. Methylene blue provides behavioral and metabolic neuroprotection against optic neuropathy. *Neurotox Res* 15: 260–273, 2009.
49. Rotschild T, Nandgaonkar BN, Yu K, Higgins RD. Dexamethasone reduces oxygen induced retinopathy in a mouse model. *Pediatr Res* 46: 94–100, 1999.
50. Russell GA, Cooke RW. Randomised controlled trial of allopurinol prophylaxis in very preterm infants. *Arch Dis Child Fetal Neonatal Ed* 73: F27–F31, 1995.
51. Serrano J, Utenthal LO, Martinez A, Fernandez AP, Martinez de Velasco J, Alonso D, Bentura ML, Santacana M, Gallardo JR, Martinez-Murillo R, Cuttitta F, Rodrigo J. Distribution of adrenomedullin-like immunoreactivity in the rat central nervous system by light and electron microscopy. *Brain Res* 853: 245–268, 2000.
52. Shankaran S. The postnatal management of the asphyxiated term infant. *Clin Perinatol* 29: 675–692, 2002.
53. Sparicio D, Landoni G, Zangrillo A. Angiotensin-converting enzyme inhibitors predispose to hypotension refractory to norepinephrine but responsive to methylene blue. *J Thorac Cardiovasc Surg* 127: 608, 2004.
54. Thachil J. Nitric oxide and adverse events of vascular endothelial growth factor inhibitors. *Curr Med Res Opin* 27: 1503–1507, 2011.
55. Tombran-Tink J, Barnstable CJ. PEDF: a multifaceted neurotrophic factor. *Nat Rev Neurosci* 4: 628–636, 2003.
56. Wanek J, Teng PY, Blair NP, Shahidi M. Inner retinal oxygen delivery and metabolism under normoxia and hypoxia in rat. *Invest Ophthalmol Vis Sci* 54: 5012–5019, 2013.
57. Wilkinson-Berka JL, Alousis NS, Kelly DJ, Gilbert RE. COX-2 inhibition and retinal angiogenesis in a mouse model of retinopathy of prematurity. *Invest Ophthalmol Vis Sci* 44: 974–979, 2003.
58. Wright RO, Lewander WJ, Woolf AD. Methemoglobinemia: etiology, pharmacology, and clinical management. *Ann Emerg Med* 34: 646–656, 1999.
59. Yamamoto R, Brecht DS, Snyder SH, Stone RA. The localization of nitric oxide synthase in the rat eye and related cranial ganglia. *Neuroscience* 54: 189–200, 1993.
60. Yiu P, Robin J, Pattison CW. Reversal of refractory hypotension with single-dose methylene blue after coronary artery bypass surgery. *J Thorac Cardiovasc Surg* 118: 195–196, 1999.
61. Younkin DP. Hypoxic-ischemic brain injury of the newborn: statement of the problem and overview. *Brain Pathol* 2: 209–210, 1992.
62. Zhang X, Rojas JC, Gonzalez-Lima F. Methylene blue prevents neurodegeneration caused by rotenone in the retina. *Neurotox Res* 9: 47–57, 2006.
63. Zhang X, Verge V, Wiesenfeld-Hallin Z, Ju G, Brecht D, Snyder SH, Hokfelt T. Nitric oxide synthase-like immunoreactivity in lumbar dorsal root ganglia and spinal cord of rat and monkey and effect of peripheral axotomy. *J Comp Neurol* 335: 563–575, 1993.
64. Ziche M, Morbidelli L. Nitric oxide and angiogenesis. *J Neurooncol* 50: 139–148, 2000.